TÜBİTAK

Turkish Journal of Mathematics

http://journals.tubitak.gov.tr/math/

Research Article

Turk J Math
(2017) 41: 585 – 604

doi:10.3906/mat-1411-8

Dynamics of a predator-prey system with a mate-finding Allee effect on prey

Ruiwen WU, Xiuxiang LIU*
School of Mathematical Sciences, South China Normal University, Guangzhou, P.R. China

Received: 02.11.2014 • **Accepted/Published Online:** 25.06.2016 • **Final Version:** 22.05.2017

Abstract: We consider a predator–prey system with nonmonotonic functional response and a hyperbolic type of mate-finding Allee effect on prey. A detailed mathematical analysis of the system, including the stability and a series of bifurcations (a saddle-node, a Hopf, and a Bogdanov–Takens bifurcation), has been given. The mathematical results show that the system is highly sensitive to the parameters and initial status. It exhibits a stable limit cycle, or different types of heteroclinic curves, or a homoclinic loop when parameters take suitable values.

Key words: Predator–prey system, mate-finding Allee effect, nonmonotonic functional response, Bogdanov–Takens bifurcation, heteroclinic curve, homoclinic loop

1. Introduction

The dynamical behaviors of predator–prey systems subject to Allee effects have gained a lot of attention in the current study of mathematical biology [6, 7, 11, 13, 30]. Allee effects describe a positive relationship between (a component of) individual fitness and population density [1, 2, 32], also known as inverse density dependence, positive density dependence, or depensation and depensatory dynamics in fisheries literature. The Allee effect implies a scenario in which, at low densities, a population subject to an Allee effect may go to extinction; thus, the study of predator–prey systems subject to Allee effects has a profound significance on conservation [14, 18, 19], the management of endangered species [10], biological invasions [6, 8], pest control [17], etc.

A range of mechanisms may lead to Allee effects, including broadcast spawning, pollen limitation, and cooperative breeding. One can refer to [9] for further information. Among them, mate-finding is the most famous; it is hard to find any studies on Allee effects without mentioning it. Individuals in a population fail to find a suitable mate during their reproductive period at low density, thus resulting in reduced reproductive outputs, and then a mate-finding Allee effect may arise. Examples include the Glanville fritillary butterfly, sheep ticks, and whales [9]. Mathematically, a mate-finding process can be modeled by the female mating rate $R(N)$ that satisfies [5, 9]

$$R(N) = 0,\ R'(N) > 0,\ \text{and}\ \lim_{N\to+\infty} R(N) = 1,$$

where N is the population size or density. Some frequently used $R(N)$ models are as follows:

$$R(N) = 1 - e^{-\frac{N}{\theta}},\ R(N) = 1 - (1-\xi)^{\eta N},\ R(N) = 1 - (1-\xi)e^{-\frac{N}{\theta}}\ (0\ at\ N = 0),$$

*Correspondence: liuxx@scnu.edu.cn
2010 *AMS Mathematics Subject Classification:* 92D25 34D05 34C60.
This work was supported in part by the NSF of Guangdong Province (S20120100 - 10034 and No. 2016A030313426)

with $0 < \xi < 1$ and $\theta, \eta > 0$. Their biological explanations can be found in [5, 9, 12]. In our study, we are interested in the following hyperbolic form:

$$R(N) = \frac{N}{N+\theta},$$

which was proposed by Dennis [12]. Parameter $\theta > 0$ represents the mate-finding Allee effect strength. If θ gets higher, the mate-finding Allee effect gets stronger. A general predator–prey system with the prey population subject to the hyperbolic type of mate-finding Allee effects can be written as

$$\begin{cases} \dfrac{\mathrm{d}N}{\mathrm{d}\tau} = BN\dfrac{N}{N+\theta} - DN(1+\dfrac{N}{K}) - F(N)P, \\ \dfrac{\mathrm{d}P}{\mathrm{d}\tau} = eF(N)P - MP, \end{cases} \tag{1}$$

where $N(\tau)$ and $P(\tau)$ are densities of prey and predator, respectively, and B and D denote the per capita birth rate and death rate of prey, respectively. K is the prey environment carrying capacity, e characterizes the conversion efficiency, and M is intrinsic mortality of predators. We assume that B, D, K, e, $M > 0$. The functional response $F(N)$ is assumed to satisfy the following:

(A1) $F(N)$ is differentiable in $N \in [0, +\infty)$,

(A2) $F(0) = 0$, $F(N) > 0$ for $N > 0$.

Many types of functional response satisfy the above assumptions, such as αN, $\frac{\alpha N}{N+\gamma}$, $\frac{\alpha N}{N^2+\beta N+\gamma}$, $\beta N e^{-\alpha N}$, with α, β, $\gamma > 0$. Here we focus on the nonmonotonic functional response

$$F(N) = \frac{CN}{N^2 + A},$$

which was introduced by Sokol and Howell [31] and studied by many other authors, such as Xiao and Ruan [29, 34], Olivares et al. [26, 27], and Jiang and Song [20]. Parameters C and $\sqrt{A}$ represent the per capita attack rate and the number of prey at which the predation rate is maximal. Obviously, $F(N)$ satisfies (A1) and (A2). More precisely, we consider the following system:

$$\begin{cases} \dfrac{\mathrm{d}N}{\mathrm{d}\tau} = BN\dfrac{N}{N+\theta} - DN(1+\dfrac{N}{K}) - \dfrac{CNP}{N^2+A}, \\ \dfrac{\mathrm{d}P}{\mathrm{d}\tau} = \dfrac{eCNP}{N^2+A} - MP, \end{cases} \tag{2}$$

In order to reduce the number of parameters from eight to five, we rescale

$$x = \frac{N}{K},\ y = \frac{CP}{BK^2},\ t = B\tau,$$

and set

$$\delta = \frac{\theta}{K},\ d = \frac{D}{B},\ a = \frac{A}{K^2},\ \varepsilon = \frac{eC}{BK},\ m = \frac{M}{B},$$

where $\delta > 0$ denotes the relative strength of the mate-finding Allee effect, to obtain

$$\begin{cases} \dfrac{\mathrm{d}x}{\mathrm{d}t} = \dfrac{x^2}{\delta + x} - dx(1+x) - \dfrac{xy}{x^2+a} := f_1(x,y), \\ \dfrac{\mathrm{d}y}{\mathrm{d}t} = \dfrac{\varepsilon xy}{x^2+a} - my := f_2(x,y). \end{cases} \tag{3}$$

Note that $B > D > 0$, so $0 < d < 1$. We assume that $0 < d < 1$ holds in our study or else both prey and predator populations will go extinct, and other parameters are positive, i.e. δ, a, ε, $m > 0$.

In this study, we first summarize two general results of predator–prey systems with a hyperbolic type of mate-finding Allee effect on prey, i.e. system (1). Then we aim to explore the dynamics of such systems by considering a specific functional response (referred to system (3)). An almost complete qualitative and bifurcation analysis of system (3) is presented, including the stability properties of the equilibria, the existence of limit cycles, a saddle-node and a Hopf bifurcation of codimension 1, and a Bogdanov–Takens bifurcation of codimension 2. Moreover, it exhibits a complex diversity of the stability of boundary equilibria and the existence of interior equilibria, a stable limit cycle, or different types of heteroclinic curves, or a homoclinic loop. We propose a simple and useful sufficient condition to prove that the new system can undergo a supercritical Hopf bifurcation. As the prey population could be very vulnerable because of the mate-finding Allee effect, we consider the predator mortality rate as the bifurcation parameter and we know that the mortality of the predator could mitigate the negative effects caused by Allee effects, though extinction is always a potential threat to the system.

We organize the paper as follows. Two main mathematical features of system (1), the existence and stability of boundary and interior equilibria of system (3), and their bifurcation analysis are presented in Sections 2 and 3. A discussion is given in Section 4. Numerical examples are carried out in different sections to support our findings.

2. The existence and stability of equilibria

2.1. Two general mathematical results of system (1)

The following theorem indicates that system (1) always has a stable extinction equilibrium E_0.

Theorem 2.1 *Assume that (A1) and (A2) are satisfied. The equilibrium E_0 of system (1) is always a stable node for all parameters.*

Since the proof is quite trivial, we omit it here. The other important mathematical feature of system (1) is the existence of nontrivial predator-free equilibria. Unlike general predator–prey systems with a logistic growth of the prey population [16, 22, 23, 25], or those subject to the most simple type of Allee effect on prey [21, 27, 30, 33], extra conditions of parameters are needed to guarantee the existence of nontrivial boundary equilibria of system (1).

Theorem 2.2 *Suppose that (A1) and (A2) hold. There exist nontrivial predator-free equilibria of system (1) if and only if $0 < \frac{D}{B} < \frac{K}{(\sqrt{K}+\sqrt{\theta})^2}$, and they appear simultaneously.*

Remark 2.1 *If $\frac{D}{B} = \frac{K}{(\sqrt{K}+\sqrt{\theta})^2}$, E_{10} and E_{20} coincide with each other and we have a unique nontrivial*

predator-free equilibrium E_{*0}. *Setting* $\theta = 0$, *that is, switching off the mate-finding Allee effect, then we have* $\frac{D}{B} < 1$, *which is consistent with the general biological assumption for predator–prey system analysis.*

2.2. Dissipativeness of system (3)

Now we will focus on system (3) for the rest of the discussion. First we define

$$q_1(x) := -dx^2 + (1 - d - d\delta)x - d\delta,\ c_1^2 = (1 - d - d\delta)^2 - 4d^2\delta,$$

and

$$q_2(x) := -mx^2 + \varepsilon x - am,\ c_2^2 = \varepsilon^2 - 4m^2 a.$$

Obviously, $\mathbb{R}^2_+ = \{(x, y)|x, y \geqslant 0\}$ is an invariant set, and there globally exists a unique solution of system (3) for any given nonnegative initial condition. The following lemma indicates that the dissipativeness of system (3) is highly associated with the death rates of both populations.

Lemma 2.1 *Let* $(x(t), y(t))$ *be a solution of system (3); then we have*

$$\limsup_{t\to+\infty} \left(x(t) + \frac{1}{\varepsilon}y(t)\right) \leqslant \frac{(1 + d - m)^2}{4dm}.$$

Proof Let $V(t) = x(t) + \frac{1}{\varepsilon}y(t)$. Differentiating V yields

$$\begin{aligned} V'(t) &= \frac{x^2}{x + \delta} - dx(1 + x) + mx - mV(t) \\ &< -dx^2 + (1 + m - d)x - mV(t) \\ &\leqslant \frac{(1 + m - d)^2}{4d} - mV(t). \end{aligned}$$

Thus, we have $\limsup_{t\to+\infty} V(t) \leqslant \frac{(1+m-d)^2}{4dm}$ and system (3) is dissipative. This completes the proof. □

2.3. The extinction equilibrium E_0

Clearly, system (3) always has an extinction equilibrium $E_0 = (0, 0)$, and $\frac{x}{x^2+a}$ satisfies the assumptions (A1) and (A2). Thus, we have the following corollary by applying Theorem 2.1 to system (3):

Corollary 2.1 *The origin* E_0 *of system (3) is always a stable node for all parameter values, with Jacobian matrix at* E_0*:*

$$J_0 = \begin{pmatrix} -d & 0 \\ 0 & -m \end{pmatrix}.$$

2.4. Nontrivial predator-free equilibria

As we have shown in Theorem 2.2, there exists distinct positive predator-free equilibria $E_{10} = (x_1, 0)$ and $E_{20} = (x_2, 0)$ of system (3) if and only if

$$0 < d(\sqrt{\delta} + 1)^2 < 1,$$

and their x-coordinates are

$$x_{10}=\frac{1}{2d}\Big(1-d-d\delta-c_1\Big),\ x_{20}=\frac{1}{2d}\Big(1-d-d\delta+c_1\Big),$$

with $1-d-d\delta>0$ and $c_1>0$. In fact, x_{10} and x_{20} are the positive roots of the equation

$$\frac{x^2}{x+\delta}-dx(1+x)=0,$$

that is

$$\frac{x}{x+\delta}\cdot q_1(x)=0,$$

since $y=0$. Moreover, $0<x_{10}<x_{20}$, and they appear simultaneously.

The stability of predator-free equilibria depends on the Jacobian matrix evaluated at E_{i0} $(i=1,2)$:

$$J_{i0}=\begin{pmatrix}\frac{\delta x_{i0}}{(x_{i0}+\delta)^2}-dx_{i0} & -\frac{x_{i0}}{x_{i0}^2+a}\\ 0 & \frac{q_2(x_{i0})}{x_{i0}^2+a}\end{pmatrix}.$$

The corresponding eigenvalues are

$$\lambda_1^{(i)}=\frac{x_{i0}}{(x_{i0}+\delta)^2}\Big[\delta-d(x_{i0}+\delta)^2\Big],\ \lambda_2^{(i)}=\frac{q_2(x_{i0})}{x_{i0}^2+a}\ (i=1,2).$$

By evaluating $\sqrt{\delta}-\sqrt{d}(x_{i0}+\delta)$ $(i=1,2)$, we get $\lambda_1^{(1)}>0$ and $\lambda_1^{(2)}<0$. Then we state the results concerning the diversified stability of E_{10} and E_{20}.

Theorem 2.3 *Suppose* $0<d(\sqrt{\delta}+1)^2<1$.

Case I: $c_2^2\leqslant 0$, *then* $\lambda_2^{(1)}<0$, $\lambda_2^{(2)}<0$ *if* $q_2(x_{i0})\neq 0$ $(i=1,2)$, *system (3) has a saddle* E_{10} *and a stable node* E_{20}.

Case II: $c_2^2>0$, *system (3) has:*

(1) a saddle E_{10} *and a stable node* E_{20} *(Figure 1(a)a, Figure 2), or*

(2) an unstable node E_{10} *and a stable node* E_{20} *(Figure 3(c)c), or*

(3) an unstable node E_{10} *and a saddle* E_{20} *(Figure 1(b)b), or*

(4) two saddle predator-free equilibria E_{10} *and* E_{20} *(Figure 4).*

Remark 2.2 *If* $d(\sqrt{\delta}+1)^2=1$, *i.e.* $c_1=0$, E_{10} *and* E_{20} *collide with each other, which can be denoted by a saddle-node equilibrium* $E_{*0}=(x_{*0},0)$, *where* $x_{*0}=\frac{1-d-d\delta}{2d}=\sqrt{\delta}$, *and* E_{*0} *has:*

(1) a stable manifold $W^s(E_{*0})$ *if* $-m\delta+\varepsilon\sqrt{\delta}-am<0$,

(2) an unstable manifold $W^u(E_{*0})$ *if* $-m\delta+\varepsilon\sqrt{\delta}-am>0$.

In order to show that the existence of interior equilibria plays a crucial role in the stability of predator-free equilibria, the detailed discussion of Theorem 2.3 will be postponed until Section 2.5. Note that E_{10} is always unstable, which means that the prey population subject to a hyperbolic form of mate-finding Allee effect has a threshold below which the populations goes to extinction. Such a threshold is called the Allee threshold.

2.5. Interior equilibria

The existence of interior equilibria is an important part of the discussion for the predator–prey system with nonmonotonic functional response $\frac{x}{x^2+a}$. If there exists any interior equilibrium, then

$$\frac{\varepsilon x}{x^2+a} - m = 0,$$

which means

$$q_2(x) = -mx^2 + \varepsilon x - a$$

has positive root(s). Since ε, m, $a > 0$, therefore it requires

$$c_2^2 \geqslant 0,$$

which is independent of δ. Moreover, we need to solve

$$x\Big[\frac{x}{x+\delta} - d(1+x) - \frac{y}{x^2+a}\Big] = 0$$

to obtain

$$\begin{aligned} y &= \frac{x^2+a}{x+\delta}\Big[x - d(1+x)(x+\delta)\Big] \\ &= \frac{x^2+a}{x+\delta} q_1(x), \end{aligned}$$

where x is the root of equation $q_2(x) = 0$. To guarantee $y > 0$, we should also have

$$q_1(x) > 0.$$

2.5.1. $d(\sqrt{\delta}+1)^2 \geqslant 1$.

In this case, system (3) has at most one nontrivial predator-free equilibrium E_{*0} (the saddle-node equilibrium) on the x-axis except E_0. Note that $q_1(x) \leqslant 0$ for all x and thus $y \leqslant 0$ for all $x > 0$, which means no interior equilibrium would be found in the first quadrant. Moreover, E_0 is globally asymptotically stable if $d(\sqrt{\delta}+1)^2 > 1$.

2.5.2. $d(\sqrt{\delta}+1)^2 < 1$.

We know that system (3) has a stable node E_0 and two boundary equilibria E_{10} and E_{20} on x-axis in the case. We discuss the existence of interior equilibria and the stability of E_{10} and E_{20} in three cases.

Case I: $c_2^2 < 0$. From the function $q_2(x) < 0$ for all x, it follows that the equation $q_2(x) = 0$ has no positive root(s), i.e. there are no interior equilibria of system (3). Obviously, we get a saddle E_{10} and a stable node E_{20}.

Case II: $c_2^2 = 0$. There is a unique positive root $x_* = \frac{\varepsilon}{2m} = \sqrt{a}$ for equation $q_2(x) = 0$ if $c_2^2 = 0$. Besides, we should have $x_{10} < x_* < x_{20}$ to guarantee $y_* > 0$ since $q_1(x_{10}) = q_1(x_{20}) = 0$, and thus $\sqrt{a}$ is assumed to satisfy

$$x_{10} < \sqrt{a} < x_{20},$$

that is,

$$a - \frac{1-d-d\delta}{d}\sqrt{a} + \delta < 0,$$

or otherwise $y_* \leqslant 0$. Note that E_{10} is a saddle and E_{20} is a stable node if $y_* \neq 0$. $E_* = (x_*, y_*)$ could be a saddle-node point (Figure 3(a)a) or a cusp (Figure 3(b)b) of system (3). Even if the initial status is sufficient, the predator population still goes to extinction for almost initial values, and only one of the trajectories converges to E_*. More detailed results about E_* will be discussed in Section 3.

Case III: $c_2^2 > 0$. In this case, there are two positive roots x_1, x_2 of $q_2(x) = 0$, where $x_1 = \frac{\varepsilon - c_2}{2m}$ and $x_2 = \frac{\varepsilon + c_2}{2m}$. Clearly, we have $0 < x_1 < x_2$ and $0 < x_{10} < x_{20}$. For the sake of simplicity, we define

$$a_1 := \frac{1}{4m^2}\left[\varepsilon^2 - (\varepsilon - 2mx_{10})^2\right], \; a_2 := \frac{1}{4m^2}\left[\varepsilon^2 - (\varepsilon - 2mx_{20})^2\right].$$

Our results are summarized in Table. For better comprehension, a numerical simulation is illustrated in Figure 5. The proof is straightforward, so we only verify (4); others can be shown in a similar way. If $\frac{\varepsilon}{2x_{20}} < m < \frac{\varepsilon}{2x_{10}}$ and $\max\{0, a_1, a_2\} < a < \frac{\varepsilon^2}{4m^2}$, then we have $x_{10} < x_1 < x_2 < x_{20}$, and thus $q_1(x_1) > 0$, $q_1(x_2) > 0$, since $q_1(x_{10}) = q_1(x_{20}) = 0$. There exist two interior equilibria $E_1 = (x_1, y_1)$ and $E_2 = (x_2, y_2)$, where

$$x_1 = \frac{\varepsilon - c_2}{2m}, \; y_1 = \frac{x_1^2 + a}{x_1 + \delta} q_1(x_1),$$

$$x_2 = \frac{\varepsilon + c_2}{2m}, \; y_2 = \frac{x_2^2 + a}{x_2 + \delta} q_1(x_2).$$

Furthermore, if $\frac{\varepsilon}{x_{10}+x_{20}} < m < \frac{\varepsilon}{2x_{10}}$, then $\max\{0, a_1, a_2\} = a_1$ (Figure 5, domain (4(i))). If $\frac{\varepsilon}{2x_{20}} < m < \frac{\varepsilon}{x_{10}+x_{20}}$, then $\max\{0, a_1, a_2\} = a_2$ (Figure 5, domain (4(ii))). It is interesting to see that $q_2(x_{10}) < 0$, $q_2(x_2) < 0$, and then it follows that $\lambda_2^{(1)} < 0$ and $\lambda_2^{(2)} < 0$, which implies that system (3) has a saddle E_{10} and a stable node E_{20}.

Table.

	Condition	Stability of E_{10}, E_{20}	Existence of E_1, E_2
(1)	$m > \frac{\varepsilon}{2x_{10}}$, or $0 < m < \frac{\varepsilon}{2x_{20}}$	E_{10}: unstable E_{20}: depends on a	no interior equilibria Figure 1
(2)	$\frac{\varepsilon}{2x_{20}} < m < \frac{\varepsilon}{x_{10}+x_{20}}$ $a_1 < a < a_2$	E_{10}: a saddle E_{20}: a saddle	only E_1 exists Figure 4 and Figure 6
(3)	$\frac{\varepsilon}{x_{10}+x_{20}} < m < \frac{\varepsilon}{2x_{10}}$ $a_2 < a < a_1$	E_{10}: an unstable node E_{20}: a stable node	only E_2 exists Figure 3(c)c
(4)	$\frac{\varepsilon}{2x_{20}} < m < \frac{\varepsilon}{2x_{10}}$ $\max\{0, a_1, a_2\} < a < \frac{\varepsilon^2}{4m^2}$	E_{10}: a saddle E_{20}: a stable node	both E_1, E_2 exist Figure 2 and Figure 7

Remark 2.3 *If $0 < m < \frac{\varepsilon}{2x_{20}}$, or $m > \frac{\varepsilon}{2x_{10}}$, system (3) has no positive equilibrium and we also have the following:*

(i) a saddle E_{10} and a stable node E_{20} exist if $a_1 < a < \frac{\varepsilon^2}{4m^2}$ or $a_2 < a < \frac{\varepsilon^2}{4m^2}$ (Figure 1(a)a),

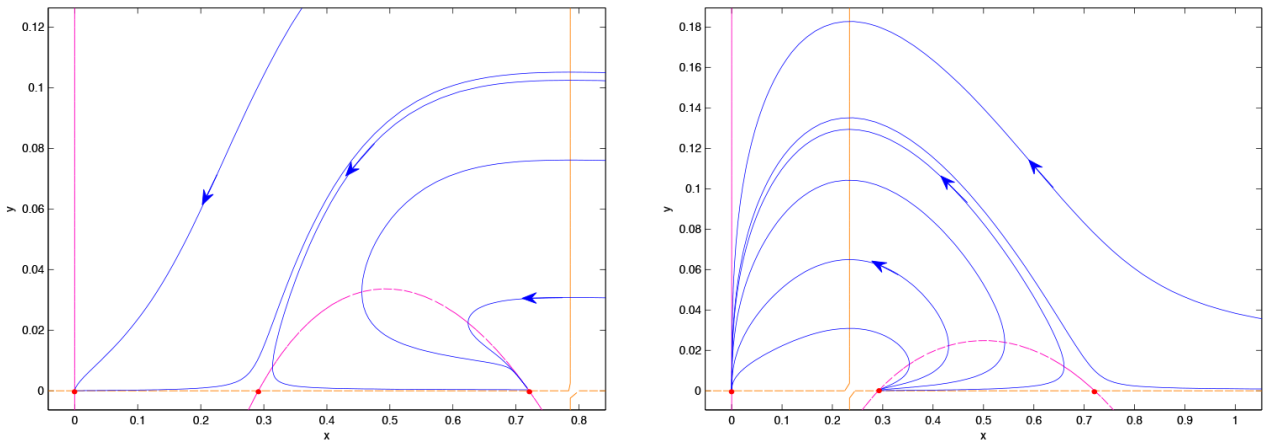

(a) $a_2 < a < \frac{\varepsilon^2}{4m^2}$ (b) $0 < a < \min\{a_1, a_2\}$

Figure 1. Phase portraits of system (3). a, ε, and m are satisfied in the Table (Condition 1), corresponding to domains (1(i)) and (1(ii)) in Figure 5. $\delta = 0.21$, $d = 0.45$, $\varepsilon = 0.56$. (a) $a = 0.9$, $m = 0.29$. (b) $a = 0.6$, $m = 0.2$.

(ii) an unstable E_{10} *or a saddle* E_{20} *exists if* $0 < a < min\{a_1, a_2\}$ *(Figure 1(b)b).*

Theorem 2.4 *Suppose* $d(\sqrt{\delta}+1)^2 < 1$ *and* $c_2^2 > 0$. E_1 *appears with a saddle* E_{10} *while* E_2 *appears with a stable node* E_{20}. *Moreover,* E_1 *is:*

(1) stable if $2x_1^3 + 3\delta x_1^2 + \delta a - (x_1+\delta)^2(3x_1^2 + 2x_1 + a)d < 0$,

(2) unstable if $2x_1^3 + 3\delta x_1^2 + \delta a - (x_1+\delta)^2(3x_1^2 + 2x_1 + a)d > 0$,

where $x_1 = \frac{\varepsilon - c_2}{2m}$. *If* E_2 *exists in the first quadrant, then it is a saddle.*

Proof The first part of the theorem follows immediately from the Table. As for the stability of E_i $(i = 1, 2)$, the Jacobian matrixes evaluated at E_i $(i = 1, 2)$ are

$$J_i = \begin{pmatrix} x_i\Big[\frac{\delta}{(x_i+\delta)^2} - d + \frac{2x_iy_i}{(x_i^2+a)^2}\Big] & -\frac{x_i}{x_i^2+a} \\ \frac{\varepsilon y_i(a-x_i^2)}{(x_i^2+a)^2} & 0 \end{pmatrix},$$

where

$$\det J_i = \frac{\varepsilon x_i y_i(a - x_i^2)}{(x_i^2+a)^3} \ (i = 1, 2),$$

and

$$\begin{aligned} \mathrm{tr}J_i &= x_i\Big[\frac{\delta}{(x_i+\delta)^2} - d + \frac{2x_iy_i}{(x_i^2+a)^2}\Big] \\ &= \frac{x_i}{(x_i+\delta)^2(x_i^2+a)}\Big[2x_i^3 + 3\delta x_i^2 + \delta a - (x_i+\delta)^2(3x_i^2 + 2x_i + a)d\Big]. \end{aligned}$$

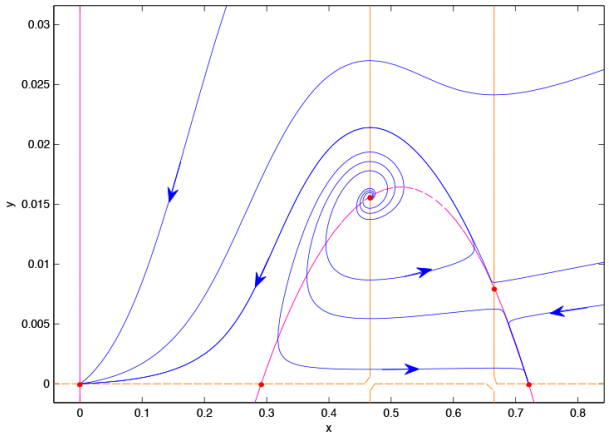

(a) An unstable E_1 and a saddle E_2

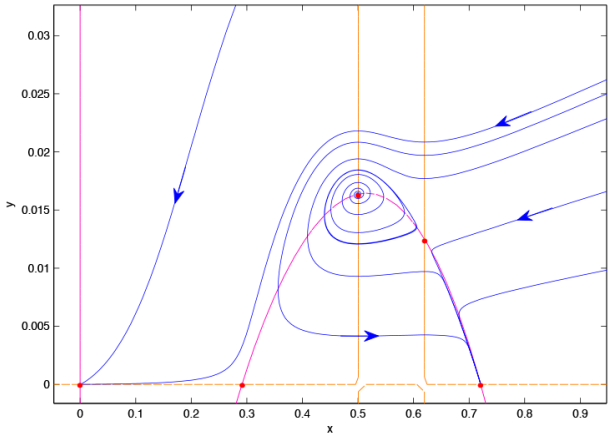

(b) A stable limit cycle and a saddle E_2

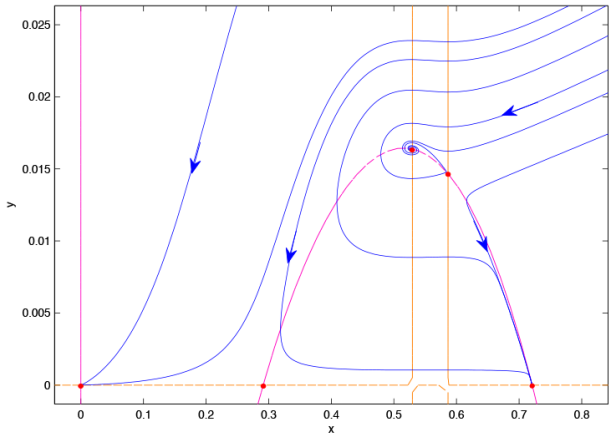

(c) A stable E_1 and a saddle E_2

Figure 2. Phase portraits of system (3). a, ε, and m are satisfied in the Table (Condition 4), corresponding to domain (4(ii)) in Figure 5. $\delta = 0.21$, $d = 0.45$, $\varepsilon = 0.56$, $a = 0.31$. (a) $m = 0.495$. (b) $m = 0.5$. (c) $m = 0.5022$.

Notice that the term $\sqrt{a} - x_i$ $(i = 1, 2)$ determines the sign of $\det J_i$ $(i = 1, 2)$, and then we have $\det J_1 > 0$, and $\det J_2 < 0$. Thus, if E_2 exists in the first quadrant, it is a saddle point, implying the existence of an unstable manifold $W^u(E_2)$ that joins E_2 and E_{20} (Figure 2, Figure 3(c)c, and Figure 7). An easy induction gives that E_1 is:

(1) stable if $2x_1^3 + 3\delta x_1^2 + \delta a - (x_1 + \delta)^2(3x_1^2 + 2x_1 + a)d < 0$,

(2) unstable if $2x_1^3 + 3\delta x_1^2 + \delta a - (x_1 + \delta)^2(3x_1^2 + 2x_1 + a)d > 0$.

This completes the proof. □

In fact, E_1 is stable if $\frac{\delta}{x_1+\delta} - d + \frac{2x_1 y_1}{(x_1^2+a)^2} < 0$, i.e. the slope of the prey isocline is negative, and it is unstable if the slope is positive.

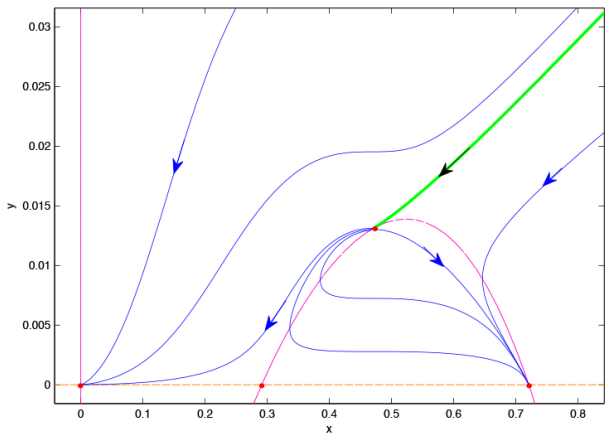

(a) A saddle-node E_*

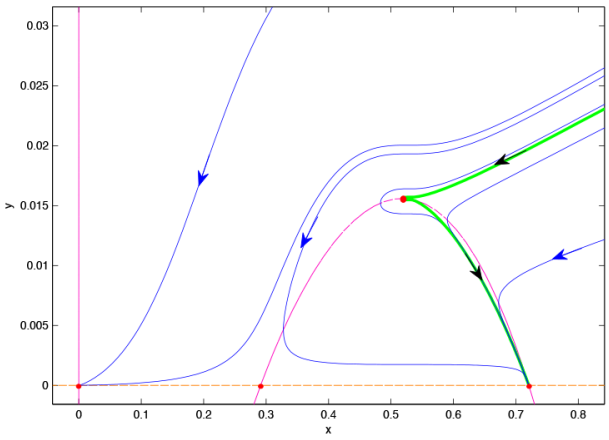

(b) A cusp E_*

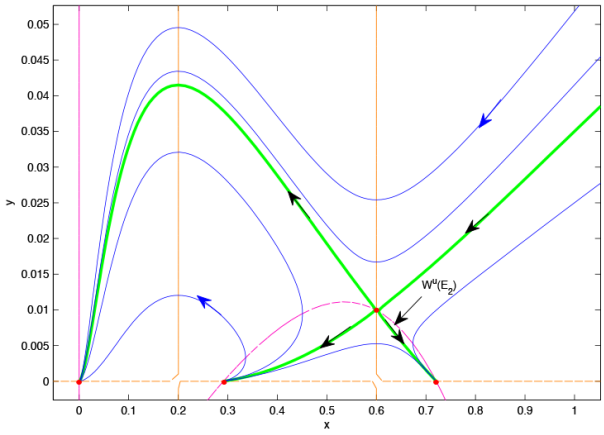

(c) A saddle E_2; a, ε, and m are satisfied in the Table (Condition 3), corresponding to domain (3) in Figure 5

Figure 3. Phase portraits of system (3). $\delta = 0.21$, $d = 0.45$, $\varepsilon = 0.56$. (a) $a = 0.22$, $m = 0.596962$. (b) $a = 0.28$, $m = 0.529150$. (c) $a = 0.12$, $m = 0.7$.

Lemma 2.2 *If $d(\sqrt{\delta}+1)^2 < 1$ and $c_2^2 > 0$, there exists a heteroclinic cycle $\tilde{\Gamma}$ in the first quadrant connecting E_{10} and E_{20} for certain δ, d, a, ε, and m, where a, ε, and m satisfy $\frac{\varepsilon}{2x_{20}} < m < \frac{\varepsilon}{x_{10}+x_{20}}$, $a_1 < a < a_2$.*

Proof We follow the idea in [26]. If $\frac{\varepsilon}{2x_{20}} < m < \frac{\varepsilon}{x_{10}+x_{20}}$, $a_1 < a < a_2$, then both E_{10} and E_{20} are saddle points. Let $W^s(E_{10})$ and $W^u(E_{20})$ represent the stable manifold of E_{10} and the unstable manifold of E_{20}, respectively. The dissipativeness of system (3) ensures that the α-limit of $W^s(E_{10})$ and ω-limit of $W^u(E_{20})$ are bounded in the direction of the y-axis as $t \to +\infty$; moreover, the stability of E_0 also guarantees that both $W^s(E_{10})$ and $W^u(E_{20})$ lie in the first quadrant.

There exists some $\tilde{x}$ where $x_{10} < \tilde{x} < x_{20}$, such that $(\tilde{x}, \tilde{y}^s) \in W^s(E_{10})$ and $(\tilde{x}, \tilde{y}^u) \in W^u(E_{20})$, where $\tilde{y}^s := y^s(\delta, d, a, \varepsilon, m)$ and $\tilde{y}^u := y^u(\delta, d, a, \varepsilon, m)$. $W^s(E_{10})$ can intersect $W^u(E_{20})$ for certain δ, d, a, ε, and m for the vector field of system (3) is continuous with respect to such parameters above, and it

follows that there exists $\tilde{\delta}$, $\tilde{d}$, $\tilde{a}$, $\tilde{\varepsilon}$, and $\tilde{m}$ such that $\tilde{y}^s = \tilde{y}^u$, i.e. $y^s(\delta, d, a, \varepsilon, m) = y^u(\delta, d, a, \varepsilon, m)$. By the existence and uniqueness theorem, such an intersection occurs with a whole trajectory $\tilde{\Gamma}_{12}$, and obviously $\tilde{\Gamma}_{12} \subset W^s(E_{10}) \cap W^u(E_{20})$. Thus, a heteroclinic cycle $\tilde{\Gamma} = E_{20} \cup \tilde{\Gamma}_{12} \cup E_{20} \cup \tilde{\Gamma}_{1020}$ exists for some suitable δ, d, a, ε, and m (Figure 6). This completes the proof. □

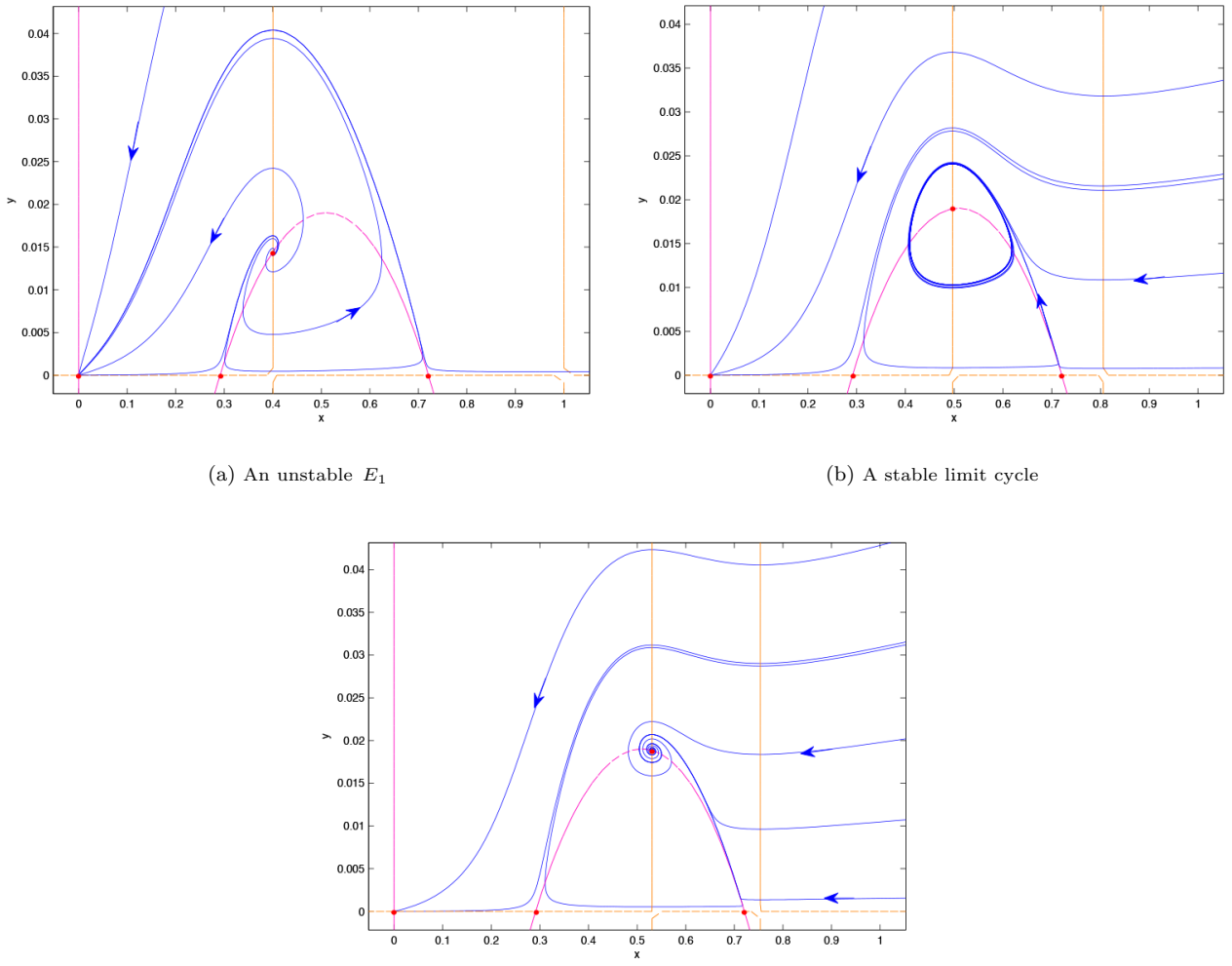

(a) An unstable E_1

(b) A stable limit cycle

(c) A stable E_1

Figure 4. Phase portraits of system (3). a, ε, and m are satisfied in the Table (Condition 2), corresponding to domain 2 in Figure 5. $\delta = 0.21$, $d = 0.45$, $\varepsilon = 0.56$, $a = 0.4$. (a) $m = 0.4$. (b) $m = 0.43$. (c) $m = 0.436$.

Remark 2.4 *Assuming* $d(\sqrt{\delta}+1)^2 < 1$, $c_2^2 > 0$, $\frac{\varepsilon}{2x_{20}} < m < \frac{\varepsilon}{x_{10}+x_{20}}$, *and* $a_1 < a < a_2$, *system (3) has only one interior equilibrium* E_1. *The unstable focus* E_1 *is surrounded by at least one limit cycle when system (3) undergoes a Hopf bifurcation if* $2x_1^3 + 3\delta x_1^2 + \delta a - (x_1+\delta)^2(3x_1^2 + 2x_1 + a)d = 0$. *The limit cycle expands (Figure 4(b)b) and finally hits the heteroclinic cycle* $\tilde{\Gamma}$ *connecting saddle* E_{10} *and saddle* E_{20} *and disappears when parameters change; for example,* m *keeps decreasing in Figure 4c–4a). As the parameters keep changing, the heteroclinic cycle* $\tilde{\Gamma}$ *is broken, and then* E_1 *becomes unstable (Figure 4(a)a).*

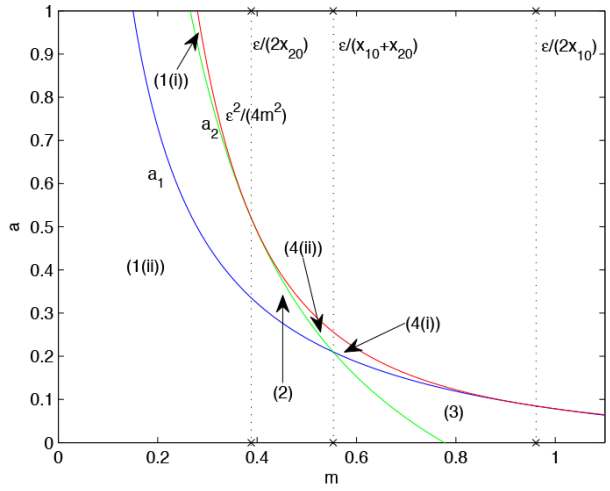

Figure 5. Bifurcation diagram of interior equilibria at (m, a). Red curve represents $a = \frac{\varepsilon^2}{4m^2}$. Blue and green curves are a_1 and a_2, respectively. Domain (i) $(i = 1, 2, 3, 4)$ corresponds to Condition (i) $(i = 1, 2, 3, 4)$ in the Table. $\delta = 0.21$, $d = 0.45$, $\varepsilon = 0.56$.

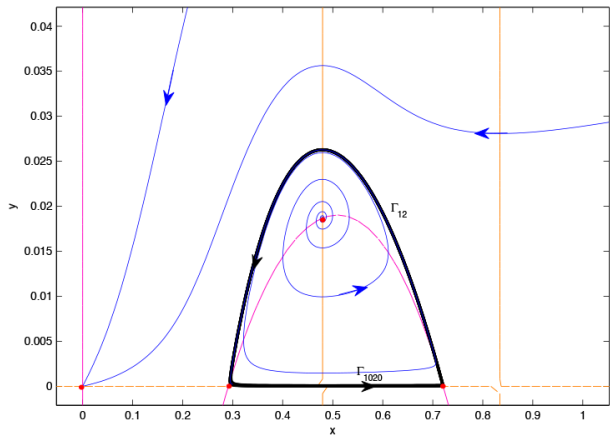

Figure 6. A heteroclinic cycle connecting saddles E_{10} and E_{20}. $\delta = 0.21$, $d = 0.45$, $a = 0.24$, $\varepsilon = 0.56$, $m = 0.42625$.

Remark 2.5 *If* $d(\sqrt{\delta}+1)^2 < 1$ *and* $c_2^2 > 0$, *and* a, ε, *and* m *satisfy* $\frac{\varepsilon}{2x_{20}} < m < \frac{\varepsilon}{2x_{10}}$, $max\{0, a_1, a_2\} < a < \frac{\varepsilon^2}{4m^2}$, *the dynamics of system (3) could be very complicated. It has five equilibria: two stable nodes* E_0 *and* E_{20}, *two saddles* E_{10} *and* E_2, *and an* E_1 *whose stability depends on* trJ_1. *In such a case, system (3) always has a heteroclinic curve connecting* E_2 *and* E_{20} *(Figure 7,* $W^u(E_2)$, *green curve). Moreover, there may exist a stable limit cycle with an unstable* E_1 *inside (Figure 2(b)b), or different heteroclinic curves joining* E_1 *and* E_2 *(Figure 7(a)a,* Γ_{12}, *dark dashed curve),* E_1 *and* E_{20} *(Figure 7(a)a,* Γ_{120}, *dark dashed curve), or joining* E_1 *and* E_{20}, E_2 *and* E_{10} *(Figure 7(b)b,* Γ_{102}, *dark dashed curve), or a stable homoclinic loop (Figure 7(c)c) when* δ, d, a, ε, *and* m *take suitable values.*

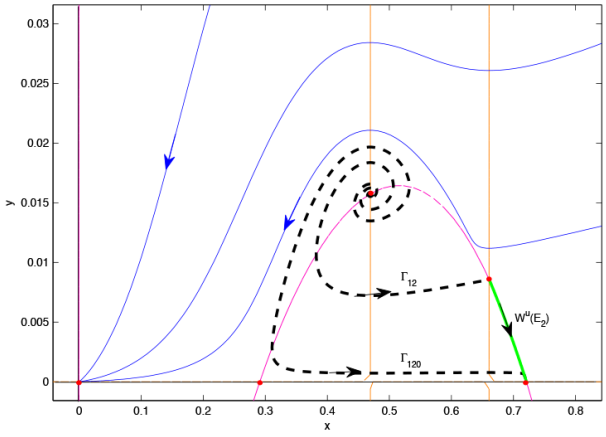

(a) Heteroclinic curves connecting E_1 and E_2 (Γ_{12}), E_1 and E_{20} (Γ_{120}), E_2 and E_{20} ($W^u(E_2)$)

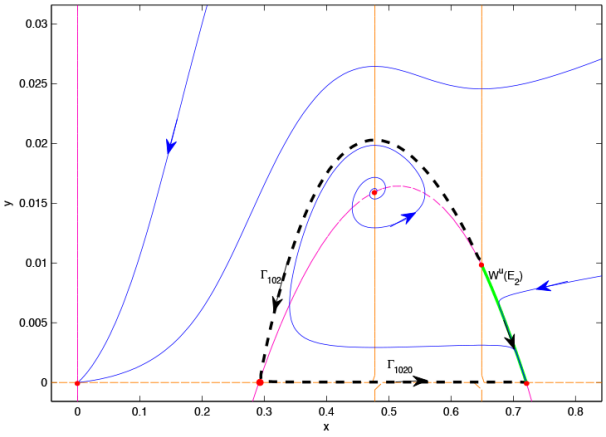

(b) Heteroclinic curves connecting E_1 and E_{20}, E_2 and E_{10} (Γ_{102}), E_2 and E_{20} ($W^u(E_2)$)

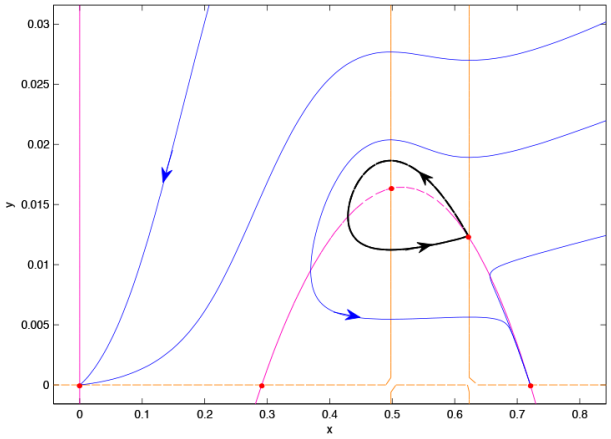

(c) Homoclinic loop

Figure 7. Different heteroclinic or homoclinic curves. $\delta = 0.21$, $d = 0.45$, $\varepsilon = 0.56$, $a = 0.31$. (a) $m = 0.4956$. (b) $m = 0.49698$. (c) $m = 0.4997$.

3. bifurcation analysis

3.1. Hopf bifurcation analysis

Suppose $0 < d(\sqrt{\delta}+1)^2 < 1$. From the discussion in Section 3, we know that a Hopf bifurcation may occur around the interior equilibrium $E_1 = (x_1, y_1)$ of system (3). Here we consider m as the bifurcation parameter. The following assumptions are used to guarantee the existence of a Hopf bifurcation:

(B1) $hp_1 := 4am^2 - \varepsilon^2$, $hp_1 < 0$,

(B2) $hp_2 := d(\varepsilon - c_2)^2 - 2m(1 - d - d\delta)(\varepsilon - c_2) + 4\delta dm^2$, $hp_2 < 0$,

(B3) $\exists m_h > 0$, s.t. $\mathrm{tr}J_1(m_h) = 0$ and $\frac{\mathrm{d}\mathrm{tr}J_1}{\mathrm{d}m}\big|_{m=m_h} \neq 0$.

Figure 8 shows the above assumptions corresponding to the Hopf bifurcations occurring in Figure 2 and Figure 4 numerically. Assumptions (B1), (B2), and (B3) are characterized by the blue, green, and red curves, respectively. We need (B1) and (B2) to guarantee the positivity of x_1 and y_1; thus, we are only interested in those m where $m_1 < m < m_2$.

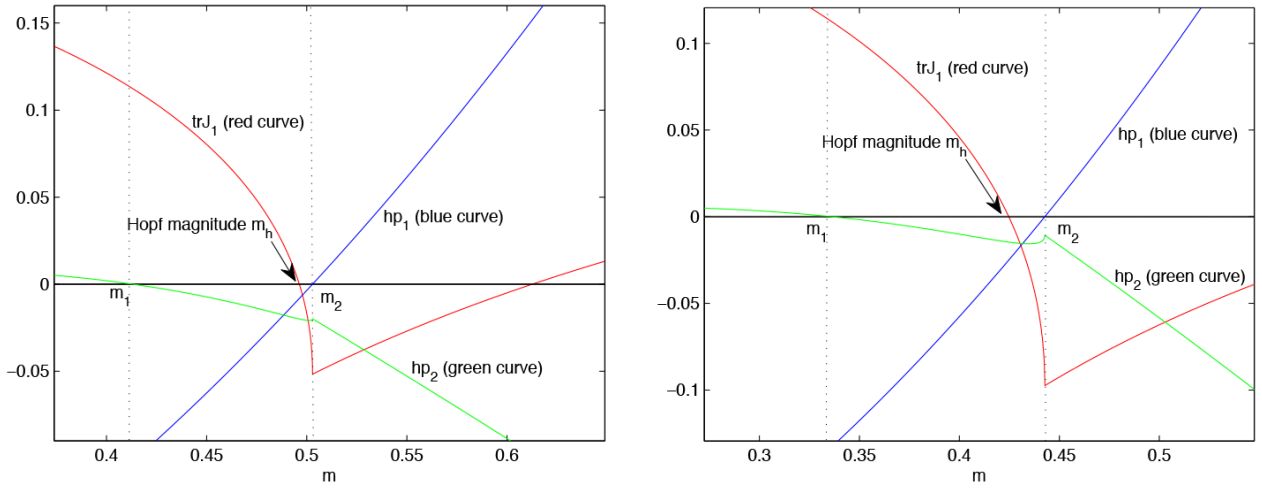

(a) Assumptions of m corresponding to Figure 2

(b) Assumptions of m corresponding to Figure 4

Figure 8. Assumptions of m to ensure the existence of a Hopf bifurcation. $\delta = 0.21$, $d = 0.45$, $\varepsilon = 0.56$. (a) $a = 0.31$. (b) $a = 0.4$.

Our next task is to discuss the stability of the limit cycle as a Hopf bifurcation occurs by computing the first Lyapunov coefficient. We translate $E_1 = (x_1, y_1)$ to the origin by making $X = x - x_1$, $Y = y - y_1$, and then we get

$$\begin{cases} \dot{X} = a_{10}X + a_{01}Y + a_{20}X^2 + a_{11}XY + a_{02}Y^2 + a_{30}X^3 \\ \qquad +a_{21}X^2Y + a_{12}XY^2 + a_{03}Y^3 + G_1(X,Y), \\ \dot{Y} = b_{10}X + b_{01}Y + b_{20}X^2 + b_{11}XY + b_{02}Y^2 + b_{30}X^3 \\ \qquad +b_{21}X^2Y + b_{12}XY^2 + b_{03}Y^3 + G_2(X,Y), \end{cases} \tag{4}$$

where

$$a_{10} = \frac{x_1\delta}{(x_1+\delta)^2} + \frac{2x_1^2y_1}{(x_1^2+a)^2} - dx_1,\ a_{01} = -\frac{x_1}{x_1^2+a},$$

$$a_{20} = \frac{\delta^2}{(x_1+\delta)^3} - \frac{x_1^3y_1 - 3ax_1y_1}{(x_1^2+a)^3} - d,\ a_{11} = \frac{x_1^2-a}{(x_1^2+a)^2},$$

$$a_{02} = 0,\ a_{30} = -\frac{\delta^2}{(x_1+\delta)^4} + \frac{x_1^4y_1 + a^2y_1 - 6ax_1^2y_1}{(x_1^2+a)^4},$$

$$a_{21} = -\frac{x_1^3 - 3ax_1}{(x_1^2+a)^3},\ a_{12} = 0,\ a_{03} = 0,$$

$$b_{10}=-\frac{\varepsilon x_1^2y_1-a\varepsilon y_1}{(x_1^2+a)^2},\ b_{01}=0,$$

$$b_{20}=\frac{\varepsilon x_1^3y_1-3a\varepsilon x_1y_1}{(x_1^2+a)^3},\ b_{11}=-\frac{\varepsilon x_1^2-a\varepsilon}{(x_1^2+a)^2},$$

$$b_{02}=0,\ b_{30}=-\frac{\varepsilon x_1^4y_1-6a\varepsilon x_1^2y_1+a^2\varepsilon y_1}{(x_1^2+a)^4},$$

$$b_{21}=\frac{\varepsilon x_1^3-3a\varepsilon x_1}{(x_1^2+a)^3},\ b_{12}=0,\ b_{03}=0,$$

and $G_i(X,Y)$ $(i=1,2)$ are C^∞ functions in (X,Y) with X^jY^k satisfying $j+k\geqslant 4$.
Then we let

$$x=X,$$

$$y=-\frac{a_{10}X}{\mu}-\frac{a_{01}Y}{\mu},$$

where $\mu^2:=\det J_1=-a_{01}b_{10}>0$, which we have discussed in Section 2. Furthermore, we have $y=-a_{01}Y/\mu$ since $\mathrm{tr}J_1=0$, i.e. $a_{10}=0$. System (4) becomes

$$\begin{cases}\dot{x}=-\mu y+g_1(x,y)+\tilde{G}_1(x,y),\\ \dot{y}=\mu x+g_2(x,y)+\tilde{G}_2(x,y),\end{cases}\tag{5}$$

where

$$g_1(x,y)=a_{20}x^2-\frac{a_{11}\mu}{a_{01}}xy+a_{30}x^3-\frac{a_{21}\mu}{a_{01}}x^2y,$$

$$g_2(x,y)=-\frac{a_{01}b_{20}}{\mu}x^2+b_{11}xy-\frac{a_{01}b_{30}}{\mu}x^3+b_{21}x^2y,$$

and $\tilde{G}_i(X,Y)$ $(i=1,2)$ are C^∞ functions in (x,y) with x^jy^k satisfying $j+k\geqslant 4$. For simplicity, we denote

$$\hat{G}_1(x,y):=g_1(x,y)+\tilde{G}_1(x,y),$$

$$\hat{G}_2(x,y):=g_2(x,y)+\tilde{G}_2(x,y).$$

The first Lyapunov coefficient σ (as defined in [15]) is given by

$$\begin{aligned}\sigma&=\frac{1}{16}\Big(\hat{G}_{1xxx}+\hat{G}_{1xyy}+\hat{G}_{2xxy}+\hat{G}_{2yyy}\Big)\\&\quad+\frac{1}{16\mu}\Big(\hat{G}_{1xy}(\hat{G}_{1xx}+\hat{G}_{1yy})-\hat{G}_{2xy}(\hat{G}_{2xx}+\hat{G}_{2yy})-\hat{G}_{1xx}\hat{G}_{2xx}+\hat{G}_{1yy}\hat{G}_{2yy}\Big)\\&=\frac{1}{8}\Big(3a_{30}-\frac{a_{11}a_{20}}{a_{01}}-\frac{2a_{20}b_{20}}{b_{10}}\Big)\end{aligned}$$

where $\hat{G}_{1xxx}:=\frac{\partial^3\hat{G}_1}{\partial x^3}\Big|_{(0,0)}$, etc. We have to admit that the expression of σ is very complicated; we fail to discuss the sign of σ directly though a stable limit cycle can be found numerically (Figure 4(b)b and Figure 2(b)b), and therefore we would like to propose a more simple but useful sufficient condition to show that $\sigma<0$.

Lemma 3.1 *Suppose that* $d(\sqrt{\delta}+1)^2<1$, $c_2^2>0$, *and (B1)–(B3) hold. If*

$$2c_2-\varepsilon<0,$$

$$3c_2^2-\varepsilon c_2-\varepsilon^2<0,$$

where $c_2=\sqrt{\varepsilon^2-4am^2}$, *then system (3) can exhibit a supercritical Hopf bifurcation when* m *passes through* m_h, *where* m_h *denotes the critical value, and a stable limit cycle appears around* $E_1=(x_1,y_1)$ *of system (3).*

The proof is only a process of elementary computations, so we do not show it here. Our numerical simulation supports our conclusion. In Figure 8(b)b, for $\delta=0.21$, $d=0.45$, $a=0.40$, $\varepsilon=0.56$, $m_h=0.43259$, we have $2c_2-\varepsilon=-0.33774<0$, $3c_2^2-\varepsilon c_2-\varepsilon^2=-4.81908<0$, and the first Lyapunov coefficient $\sigma=-0.32191$. In Figure 8(a)a, for $\delta=0.21$, $d=0.45$, $a=0.31$, $\varepsilon=0.56$, $m_h=0.499884$, we have $2c_2-\varepsilon=-0.43976<0$, $3c_2^2-\varepsilon c_2-\varepsilon^2=-0.33642<0$, and the first Lyapunov coefficient $\sigma=-7.91937$.

3.2. Saddle-node bifurcation analysis

We know that when δ_*, d_*, a_*, ε_*, m_* satisfy the following:

(C1) $d(\sqrt{\delta}+1)^2<1$,

(C2) $\varepsilon^2=4am^2$,

(C3) $a-\frac{1-d-d\delta}{d}\sqrt{a}+\delta<0$, or $\frac{\varepsilon^2}{4m^2}-\frac{1-d-d\delta}{d}\cdot\frac{\varepsilon}{2m}+\delta<0$,

then system (3) has a unique interior equilibrium $E_*=(x_*,y_*)$, and the Jacobian matrix at E_* is

$$J_*=\begin{pmatrix} x_*\left[\frac{\delta_*}{(x_*+\delta_*)^2}-d_*+\frac{2x_*y_*}{(x_*^2+a_*)^2}\right] & -\frac{x_*}{x_*^2+a_*} \\ 0 & 0 \end{pmatrix},$$

and obviously $\det J_*=0$.

In this subsection, we assume that $\mathrm{tr}J_*\neq 0$, i.e. $\frac{\delta_*}{(x_*+\delta_*)^2}-d_*+\frac{2x_*y_*}{(x_*^2+a_*)^2}\neq 0$. Now we will show that system (3) can experience a saddle-node bifurcation at E_* by Sotomayor's theorem [28], and again m is considered as the bifurcation parameter.

Therefore, we have the following conclusion.

Theorem 3.1 *Assume that (C1)–(C3) hold, and* $trJ_*\neq 0$. *System (3) can undergo a saddle-node bifurcation at* $E_*=(x_*,y_*)$ *as the parameter* m *passes through* $m=m_*$ *in the small neighborhood of* m.

3.3. Bogdanov–Takens bifurcation analysis

We have mentioned $\det J_*=0$; here we are interested in the case of $\mathrm{tr}J_*=0$, i.e., $\frac{\delta_*}{(x_*+\delta_*)^2}-d_*+\frac{2x_*y_*}{(x_*^2+a_*)^2}=0$. The following theorem aims to show that system (3) can exhibit a Bogdanov–Takens bifurcation around E_*.

Theorem 3.2 *Assume that (C1)–(C3) hold, and* $trJ_*(\delta_*,m_*)=0$. *The unique interior equilibrium* E_* *is a cusp of codimension 2, and system (3) undergoes a Bogdanov–Takens bifurcation around* E_* *when* $(\delta,m)=(\delta_*,m_*)$.

We proceed as in [24, 29]. After a series of transformations, we obtain the normal form of the Bogdanov–Takens bifurcation:

$$\begin{cases} \dot{u} = v, \\ \dot{v} = \gamma_1 + \gamma_2 v + u^2 - \gamma_3 uv + \tilde{R}, \end{cases} \tag{6}$$

where

$$\gamma_1 = \frac{x_* y_*}{(x_*^2 + a_*) Z_0(0,0,0)} r_2 + \tilde{\rho}_1,$$

$$\gamma_2 = \frac{1}{\sqrt{Z_0(0,0,0)}} \Big[\frac{x_*^2 - \delta_* x_*}{(x_* + \delta_*)^3} r_1 - r_2 \Big] + \tilde{\rho}_2,$$

$$\gamma_3 = \frac{2}{\sqrt{Z_0(0,0,0)}} \Big[\frac{x_* \delta_*}{(x_* + \delta_*)^3} + \frac{x_* y_*}{(x_*^2 + a_*)^2} \Big] + \tilde{\rho}_3,$$

$$Z_0(0,0,0) = \frac{\varepsilon x_*^2 y_*}{(x_*^2 + a_*)^3} \neq 0,$$

and (r_1, r_2) is in the small neighborhood of (δ_*, m_*), $\tilde{\rho}_i$ $(i = 1,2,3)$, and $\tilde{R}$ are smooth functions.

Remark 3.1 *We have the following conclusions by the theorems in [3, 4, 28, 29]:*

(1) The saddle-node bifurcation curve $SN = \{(\gamma_1, \gamma_2) | \gamma_1 = 0,\ \gamma_2 \neq 0\}$.

(2) The Hopf bifurcation curve

$$H = \Big\{ (\gamma_1, \gamma_2) | \gamma_2 = -2 \Big[\frac{x_* \delta_*}{(x_* + \delta_*)^3} + \frac{x_* y_*}{(x_*^2 + a_*)^2} \Big] \sqrt{-Z_0(0,0,0)\gamma_1},\ \gamma_1 < 0 \Big\}.$$

(3) The homoclinic bifurcation curve

$$HL = \Big\{ (\gamma_1, \gamma_2) | \gamma_2 = -\frac{10}{7} \Big[\frac{x_* \delta_*}{(x_* + \delta_*)^3} + \frac{x_* y_*}{(x_*^2 + a_*)^2} \Big] \sqrt{-Z_0(0,0,0)\gamma_1},\ \gamma_1 < 0 \Big\}.$$

4. Discussion

In this study, we have summarized two main mathematical features of predator–prey systems with a hyperbolic type mate-finding Allee effect, which exhibit prey-dependent functional response, and we investigated a specific system with nonmonotonic functional response. Apart from exploring the ecological interaction between prey and predator populations affected by a mate-finding Allee effect on prey mathematically, more importantly, we try to figure out how to mitigate the negative effects caused by Allee effects by changing other system parameters.

The hyperbolic type of mate-finding Allee effects on predator–prey systems directly results in the ever-present stable extinction equilibrium E_0 and extra requirements of system parameters for the existence of nontrivial predator-free equilibria. Moreover, if such equilibria exist, they appear simultaneously and the lower one (referred to as E_{10}) is unstable (Allee threshold). The stable extinction equilibrium E_0 indicates that such a system always faces a risk of extinction once the prey population drops below a certain number (Allee

threshold), and the whole system goes to extinction inevitably. Though Theorems 2.1 and 2.2 only concern predator–prey systems subject to mate-finding Allee effects with prey-dependent functional response, we believe that similar conclusions still hold for those with predator-dependent functional response.

The discussion for the existence of interior equilibria is an important concept in the study of predator–prey systems with nonmonotonic functional response $\frac{x}{x^2+a}$ [27, 29]. On one hand, the existence of interior equilibria is subject to equation $q_2(x)=0$ and function $q_1(x)$ where x_{i0} $(i=1,2)$ (x-coordinates of E_{i0} $(i=1,2)$) are positive roots of $q_1(x)=0$. On the other hand, the stability of E_{i0} $(i=1,2)$ depends on function $q_2(x)$. The mainly dynamical behaviors of system (3) could be divided into the following: (1) both populations go extinct; (2) the prey population could survive as long as its initial status starts above some certain value, while the predator population still goes to extinction, and such scenario corresponds to the existence of an unstable E_{10} and a stable node E_{20}; (3) both populations could coexist at a stable E_1 or the unique equilibrium E_*; (4) populations oscillate around E_1 implying the existence of a stable limit cycle. There also exist different types of heteroclinic curves or a stable homoclinic loop. System (3) can exhibit complicated and diverse stability of nontrivial predator–prey equilibria and existence of interior equilibria under different conditions; however, both types of equilibria do not show any global stability since E_0 is always stable. Similar results could be found in [35], as well.

If the prey population faces a mate-finding Allee effect, it usually means a high possibility of extinction for the population itself and any tiny changes may cause extinction; in other words, the prey population is vulnerable. Thus, from the applied ecological perspective, we consider the death rate of predator population m as the bifurcation parameter instead of just focusing on δ only, as m is more controllable. First, we require $c_2^2>0$, i.e. $0<m<\frac{\varepsilon}{4a}$, to ensure the existence of interior equilibria, which indicates that the predator population could establish itself if the mortality rate m drops below a certain value. A high death rate may drive the predators prone to extinction. However, from the Table, it is easy to find that low mortality of a predator population cannot always guarantee the coexistence of prey and predator populations (Figure 5, domains 1(i) and 1(ii)); the prey population quantity is not enough for the excessive numbers of the predator population and, as a result, the predator population goes faster to extinction than the prey population; there even exists a chance that the prey population could survive. Second, Figure 4 and Figures 2a–2c illustrate that a stable limit cycle could appear as m increases. If the system is in an unstable status initially, increasing m to a certain extent could translate the system from unstable to stable. The predator population suffers from a relative high mortality, thus providing an opportunity for the prey population to recover; as a result, a limit cycle may arise. Furthermore, it has been shown that system (3) may experience a series of bifurcations including the supercritical Hopf bifurcation at E_1, the saddle-node, and Bogdanov–Takens bifurcations at E_*.

From the perspective of pest control, such results imply that prey (=pest) populations may go through sustained cycles even if they suffer from mate-finding Allee effects as long as the predator population (=enemy) has a suitable m. In order to drive the prey population to extinction, a predator could be released to force the density of the prey population to decrease below the Allee threshold. We have also known that E_1 could be stable (Figure 4(c)c and Figure 2(c)c) while E_2 is always an unstable saddle; thus, system (3) enters a stable state by changing m to make the unstable E_2 vanish, which is desirable in saving endangered species and conservation.

Overall, we should be aware of such systems where a stable origin always exists, implying that extinction is a potential threat all the time, and the system itself is highly sensitive to the system parameters and the initial status. Since the parameters are of interaction and restricted mutually, we are interested in the co-3

bifurcation problem and leave it for further discussion.

Acknowledgements

The authors are very grateful to the reviewer for the careful reading and helpful comments.

References

[1] Allee WC. The Social Life of Animals. London, UK: William Heinemann, 1938.

[2] Allee WC, Emerson AE, Park O, Parkm T, Schmidt KP. Principles of Animal Ecology. Philadelphia, PA, USA: Saunders, 1949.

[3] Bogdanov R. Bifurcations of limit cycle for a family of vector fields on the plane. Selecta Math Soviet 1981; 1: 378-388.

[4] Bogdanov R. Versal deformations of a singular point on the plane in the case of zero eigenvalues. Selecta Math Soviet 1981; 1: 389-421.

[5] Boukal DS, Berec L. Single-species models of the Allee effect: extinction boundaries, sex ratios and mate encounters. J Theor Biol 2002; 218: 375-394.

[6] Boukal DS, Sabelis M, Berec L. How predator functional responses and Allee effects in prey affect the paradox of enrichment and population collapses. J Theor Biol 2007; 72: 136-147.

[7] Celik C, Duman O. Allee effect in a discrete-time predator-prey system. Chaos Solition Fract 2009; 40: 1956-1962.

[8] Chen L, Lin Z. The effect of habitat destruction on metapopulations with the Allee-like effect: a study case of Yancheng in Jiangsu Province, China. Ecol Model 2008; 213: 356-364.

[9] Courchamp F, Berec L, Gascoigne J. Allee Effects in Ecology and Conservation. Oxford, UK: Oxford University Press, 2008.

[10] Courchamp F, Clutton-Brock T, Grenfell B. Inverse density dependence and the Allee effect. Trends Ecology Evol 1999; 14: 405-410.

[11] Cui R, Shi J, Wu B. Strong Allee effect in a diffusive predator-prey system with a protection zone. J Differ Equations 2014; 256: 108-219.

[12] Dennis B. Allee effects: population growth, critical density, and the chance of extinction. Nat Res Model 1989; 3: 481-583.

[13] Graef JR, Padhi S, Pati S. Periodic solutions of some models with strong Allee effects. Nonlinear Anal Real World Appl 2012; 13: 569-581.

[14] Greene CM. Habitat selection reduces extinction of populations subject to Allee effects. Theor Popul Biol 2003; 64: 1-10.

[15] Guckenheimer J, Holmes P. Nonlinear Oscillations, Dynamical Systems and Bifurcations of Vector Fields. New York, NY, USA: Springer-Verlag, 1983.

[16] Gupta RP, Chandra P. Bifurcation analysis of modified Lesile-Gower predator-prey model with Michaelis-Menten type prey harvesting. J Math Anal Appl 2013; 398: 278-295.

[17] Hassell MP, Varley GC. New inductive population model for insect parasites and its bearing on biological control. Nature 1969; 223: 1133-1137.

[18] Hilker FM, Langlais M, Petrovskii SV, Malchow H. A diffusive SI model with Allee effect and application to FIV. Math Biosci 2007; 206: 61-80.

[19] Hurford A, Hebblewhite M, Lewis MA. A spatially explicit model for an Allee effect: why wolves recolonize so slowly in Greater Yellowstone. Theor Popul Biol 2006; 70: 244-254.

[20] Jiang J, Song Y. Stability and bifurcation analysis of a delayed Leslie-Gower predator-prey system with nonmonotonic functional response. Abstract Appl Anal 2013; 2013: 152459.

[21] Kim C, Shi J. Existence and multiplicity of positive solutions to a quasilinear elliptic equation with strong Allee effect growth rate. Results Math 2013; 64: 165-173.

[22] Kuang Y. Rich dynamics of Gause-type ratio-dependent predator-prey systems. Fields Institute Communications 1999; 21: 325-337.

[23] Kuang Y, Beretta E. Global qualitative analysis of a ratio-dependent predator-prey system. J Math Biol 1998; 36: 389-406.

[24] Kuznetsov YA. Elements of Applied Bifurcation Theory. New York, NY, USA: Springer-Verlag, 2004.

[25] Liu X, Lou Y. Global dynamics of a predator-prey model. J Math Anal Appl 2010; 371: 323-340.

[26] Olivares EG, Yaneza B, Lorca J, Palmaa A, Flores J. Consequences of double Allee effect on the number of limit cycles in a predator-prey model. Comput Math Appl 2011; 62: 3449-3463.

[27] Olivares EG, Yaneza B, Lorca J, Palmaa A, Flores J. Uniqueness of limit cycles and multiple attractors in a Gause-type predator-prey model with nonmonotonic functional response and Allee effect on prey. Math Biosci Eng 2013; 10: 345-367.

[28] Perko L. Differential Equations and Dynamical Systems. New York, NY, USA; Springer, 2001.

[29] Ruan S, Xiao D. Global analysis in a predator-prey system with nonmonotonic functional response. SIAM J Appl Math 2001; 61: 1445-1472.

[30] Sen M, Banerjee M, Morozov A. Bifucation analysis of a ratio-dependent predator-prey model with the Allee effect. Ecol Complex 2012; 11: 12-27.

[31] Sokol W, Howell JA. Kinetics of phenol oxidation by washed cells. Biotechnol Bioeng 1980; 23: 185-190.

[32] Stephens PA, Sutherland WJ, Freckleton R. What is the Allee effect. Oikos 1999; 87: 12-27.

[33] Wang W, Zhang Y, Liu C. Analysis of a discrete-time predator-prey system with Allee effect. Ecol Complex 2011; 8: 81-85.

[34] Xiao D, Ruan S. Multiple bifurcations in a delayed predator-prey system with nonmonotonic functional response. J Differ Equations 2001; 176: 494-510.

[35] Zu J. Global qualitative analysis of a predator-prey system with Allee effect on the prey species. Math Comput Simul 2013; 94: 33-54.